SCIENTIFIC REPORTS

OPEN

SUBJECT AREAS:
INFORMATION THEORY AND COMPUTATION
CHEMICAL PHYSICS
COMPUTATIONAL METHODS

Received
23 October 2013

Accepted
12 November 2013

Published
6 December 2013

Correspondence and requests for materials should be addressed to H.P.F. (fanghaiping@sinap.ac.cn)

Ion Enrichment on the Hydrophobic Carbon-based Surface in Aqueous Salt Solutions due to Cation-π Interactions

Guosheng Shi[1], Jian Liu[1,2], Chunlei Wang[1], Bo Song[1], Yusong Tu[3], Jun Hu[1] & Haiping Fang[1]

[1]Division of Interfacial Water and Key Laboratory of Interfacial Physics and Technology, Shanghai Institute of Applied Physics, Chinese Academy of Sciences, Shanghai 201800, China, [2]Graduate School of the Chinese Academy of Sciences, Beijing, 100080, China, [3]Institute of Systems Biology, Shanghai University, Shanghai, 200444, China.

By incorporating cation-π interactions to classic all-atoms force fields, we show that there is a clear enrichment of Na^+ on a carbon-based π electron-rich surface in NaCl solutions using molecular dynamics simulations. Interestingly, Cl^- is also enriched to some extend on the surface due to the electrostatic interaction between Na^+ and Cl^-, although the hydrated Cl^--π interaction is weak. The difference of the numbers of Na^+ and Cl^- accumulated at the interface leads to a significant negatively charged behavior in the solution, especially in nanoscale systems. Moreover, we find that the accumulation of the cations at the interfaces is universal since other cations (Li^+, K^+, Mg^{2+}, Ca^{2+}, Fe^{2+}, Co^{2+}, Cu^{2+}, Cd^{2+}, Cr^{2+}, and Pb^{2+}) have similar adsorption behaviors. For comparison, as in usual force field without the proper consideration of cation-π interactions, the ions near the surfaces have a similar density of ions in the solution.

Carbon-based surfaces widely exist in both nanoscale and macroscopic materials, and most of them contain π electron-rich structures which is a hexagonal carbon ring where there are rich π electrons, such as aromatic rings in biomolecules[1], humus in the soil[2,3], polycyclic aromatic hydrocarbons in air pollutants[4–6], and graphene[7,8], carbon nanotubes[9,10], and fullerenes[11]. It has been widely reported that the accumulation of ions at carbon-based surfaces greatly impacts the properties and applications of carbon-based materials, including surface- or interface-charged behaviors[12–15], aqueous suspension and aggregation[16,17], surface modification[18,19], chemical synthesis[20,21], and the function, configuration, and stability of biological systems[22–24]. We note that, in nanoscale systems, since the total number of ions is small, the accumulation of ions at a carbon-based surface results in a clear decrease of ions in the solution and at the liquid-gas interface. This affects impact the chemical reactions and charged behaviors in the solution or at the gas-liquid interface on aerosol particles[25–32], water films on the soils in the dry environment, and aggregations of polymers/macromolecules/nanoparticles in humid environment.

The understanding of the ions accumulation on the surfaces with π electron-rich structures becomes more complex due to the discovery of the cation-π interactions in 1980's[33]. The cation-π interaction is the non-covalent interaction between a cation and a π electron-rich carbon-based structure. Basing on experiments and quantum mechanical methods computations, it has been found that cation-π interactions play important roles in various systems, including control of the structures and functions of microscale and nanoscale materials, macromolecules, and proteins[34–44].

Quantum mechanical (DFT and *ab initio*) methods usually can only compute and simulate small systems with a small number of atoms[1,34–38]. For the complex systems such as the ions in the solution, we usually use classical analysis and numerical simulations with appropriate force fields. Unfortunately, the cation-π interactions have rarely been explicitly and sufficiently considered in usual all-atoms classic force fields. In the biological systems where the π electron-rich structures (for example aromatic rings) are enriched, in present popular force fields (Amber[45], Charmm[46], and Opls[47]), cation-π interactions are mainly considered by increasing the charges of the carbon atoms in π electron-rich structures. This simple treatment leads to a stronger rejection to the anions by the carbon atoms, and enhanced interactions between the carbon atoms and surrounding water molecules, and thus, affects the configuration and aggregation of protein in the aqueous salt solution[22–24].

To the worse, although many of the most well-known nano-materials (such as graphene, nanotubes, and fullerenes) include the π electron-rich carbon-based surfaces, cation-π interactions have not been included explicitly when considering behaviors of interfacial ions on these nano-materials[48–51]. In popular classic force

fields such as Amber, Charmm, and Opls, the interactions between the ions and these π electron-rich carbon-based surfaces only include the van der Waals interaction; it is undistinguishable for the interactions between ions and carbon-based surfaces, whether the surfaces contain π electron-rich structures or not. This greatly underestimates the interactions energies between the ions and π electron-rich the carbon-based surfaces. For example, the interaction energies of a Na^+ in the solution with the graphene surface are −0.2[45], −0.9[46], and −0.2[47] kcal/mol from the classic force fields Amber, Charmm, and Opls, respectively. These values are significantly lower than the value of −16.4 kcal/mol for hydrated Na^+ in calculations with the density functional theory (DFT) methods[52]. We note that, very recently, the computation of the interactions between the π electron-rich carbon-based surfaces (graphene, nanotubes, and fullerenes) and a single ion *in vacuum* has been greatly improved by modifying a polarizable force field[53]. Due to the hydration of the ions by water molecules, this force field cannot be directly used for the study of ions at such liquid-solid interface.

In this article, based on the DFT computations, we incorporate cation-π interactions to the classic force field to study the behavior of interfacial ions on the surfaces with π electron-rich carbon-based structures in the aqueous solution. On the basis of the example of the uncharged hydrophobic graphite surface and the NaCl solutions, we show that large amounts of ions in the aqueous solution are adsorbed on the carbon-based surface with π electron-rich structures, when the cation-π interaction is explicitly account for. Interestingly, although the interaction of the hydrated Cl^- with the carbon-based surface is small, Cl^- is also enriched on the surface due to the electrostatic interaction between Na^+ and Cl^-. This difference of Na^+ and Cl^- interaction strength with carbon-based surface due to the cation-π interactions leads to more Cl^- in the solution, resulting in a significant negatively charged behavior of solution (especially for nanoscale systems). We also show that the enrichment of cations on the graphite surface is universal and that other cations (Li^+, K^+, Mg^{2+}, Ca^{2+}, Fe^{2+}, Co^{2+}, Cu^{2+}, Cd^{2+}, Cr^{2+}, and Pb^{2+}) have similar behavior as Na^+. This finding provides new insight for understanding and controlling surface-charged behaviors, and points to additional applications such as ion storage and detection, carbon nanotube-based water purification, graphene-based ion filtration, and the development of low-cost carbon-based materials for water and soil pollution from heavy metal cations.

Results and discussion

Due to strong Na^+-π interactions, the hydrated Na^+ still significantly interact with the graphite surface, although the hydration interaction reduces the Na^+-π interactions[52]. For example, the interaction energy of a Na^+ around nine water molecules at its equilibrium position, including the Na^+-π interaction, is 16.4 kcal/mol (the detailed computation can be found in the Supplementary Information). This is much larger than the value of 0.9 kcal/mol obtained if the Na^+-π interaction is neglected.

In order to quantitatively study the effect of the cation-π interaction on the ion distributions on the graphite surface, using density functional theory (DFT) (see details in the Supplementary Information), we modified the NAMD program by introducing the Na^+-π interactions. We modeled the interaction as

$$V = \varepsilon\left((z_m/z)^8 - 2(z_m/z)^4\right) \quad (1)$$

where ε and z_m are the adsorption energy and balance position distance (the vertical dimension between the Na^+ and the surface) of Na^+ on the graphite surface, respectively, and z is the distance of vertical dimension between the Na^+ and the surface. We note that the hydrated Cl^--π interaction is much smaller, which is only of ~1/10 of the hydrated Na^+-π interaction, so it is neglected in the computation.

We first consider how the hydrated Na^+-π interaction affects the distribution of Na^+ and Cl^- in the NaCl solution. Figure 1A and 1B shows a typical snapshot in which many Na^+ and Cl^- in the NaCl solution are adsorbed on the graphite surface and others are free in the bulk water. In order to obtain a quantitative description, we compute the distribution probabilities of Na^+ and Cl^- in the water along the z-direction on the graphite surface, which are shown in Figure 1C. We can see that there is a peak for Na^+ at ~0.39 nm. We also compute the average number of Na^+ at the graphite surface, which is defined as the number of Na^+ with z positions less than z_C; z_C = 0.50 nm is the location of the first valley in the Na^+ distribution, with a value of 48.0. Considering that the total number of Na^+ in the solution is only 70, it is clear that most of Na^+ is adsorbed on the graphite surface. For comparison, we also performed MD simulations with the hydrated Na^+-π interactions turned off. As shown in Figure 1C, without the hydrated Na^+-π interactions, Na^+ has a flat distribution along the z-direction.

Interestingly, there is also a peak for Cl^- even when the hydrated Cl^--π interaction is neglected. Moreover, the peak for Cl^- is located at z = 0.37 nm, which is lower than the location of the peak for Na^+, as shown in Figure 1D. Careful examination shows that the Na^+-Cl^- electrostatic interaction together with the van der Waals interaction between Cl^- and the graphite surface results in a large amount of Cl^- preferring to remain closer to the graphite surface. As with the two typical cases shown in Figure 2A and 2B, a Cl^- close to the graphite surface always has a very close neighboring Na^+, and the nearby water molecules also provide an indirect interaction between Cl^- and Na^+. Our analysis shows that the average distance between a Cl^- close to the graphite surface and the nearest Na^+ is only 0.26 nm, which is much smaller than the average distance (0.34 nm) between a Cl^- in the solution and its nearest Na^+. However, the z value of the peak for Cl^- should be larger than the z value of the peak for Na^+ if the Cl^- close to the solid surface only results from the electrostatic attraction by Na^+. We note that the Cl^- have a much stronger van der Waals interaction with the graphite surface compared to Na^+, since the Lennard-Jones (LJ) parameters are ε_{CCl} = 0.103 kcal/mol and

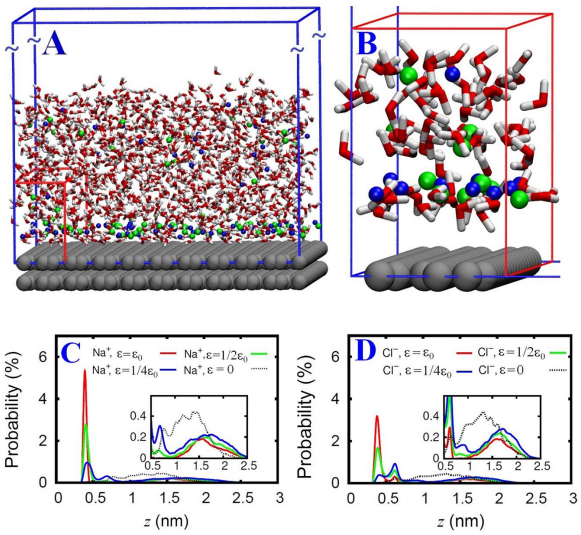

Figure 1 | Na^+ and Cl^- in the NaCl solution on the graphite surface. (A) Snapshot. (B) Close-up of the lower left corner. The gray structures depict the graphite sheets; water molecules and ions are shown with oxygen in red, hydrogen in white, Na^+ in blue, and Cl^- in green, respectively. (C and D) Distribution probabilities of Na^+ (C) and Cl^- (D) along the z-direction in the NaCl solution on the graphite surface, with the normal hydrated Na^+-π interaction (ε = ε_0, red solid line), reduced interaction of ε = ε_0/2 (green solid line) and ε = ε_0/4 (blue solid line), and without the hydrated Na^+-π interaction (ε = 0.0, black dashed line).

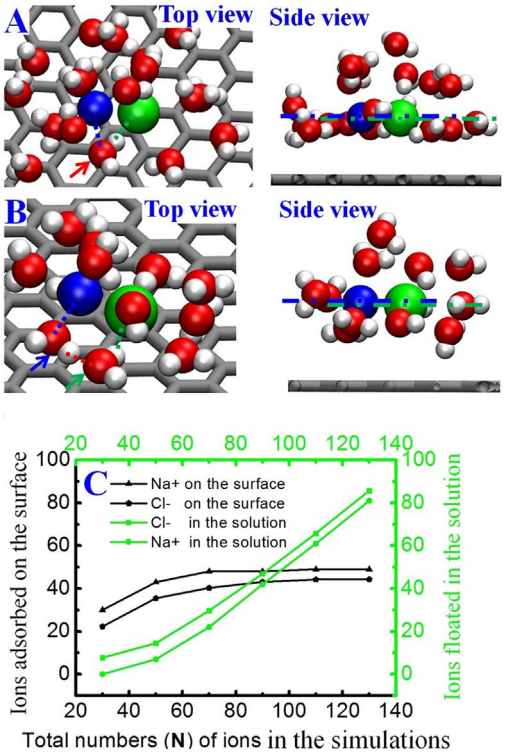

Figure 2 | Ions at the liquid-graphite interface. (A and B) Snapshots of two typical cases of a Cl^- with its neighboring Na^+ and water molecules on the graphite surface. In (A, top view), a water molecule (marked by the red arrow) directly interacts with both Na^+ and Cl^- simultaneously (the interactions are shown by blue and green dotted lines). In (B, top view), one water molecule (marked by the blue arrow and blue dotted line) interacts with Na^+, and another water molecule (marked by the green arrow and green dotted line) interacts with Cl^-. These two water molecules form a hydrogen bond (marked by the red dotted line) to bridge the indirect interaction between Na^+ and Cl^-. In the side view of (A,B), the horizontal line of the center Na^+ (blue) and Cl^- (green) are shown. The color settings are the same as in Figure 1. (C) The numbers of ions adsorbed on the graphite surface (black) and floated in the solution (green with right coordinates) with respect to the total numbers (N) of ions in the aqueous salt solution.

$\varepsilon_{CNa} = 0.057$ kcal/mol, respectively. Thus, we postulate that it is the combination of the van de Waals interaction of Cl^- with the graphite surface and the Na^+-Cl^- electrostatic interaction that makes the Cl^- accumulate closer to the graphite surface. The van der Waals distance σ_{GCl} of 0.37 nm, consistent with the z value of the peak for Cl^-, further verifies this assumption. Since the "apparent" adsorption of Cl^- by the graphite surface is mediated by the Na^+-Cl^- electrostatic interaction, the peak for Na^+ is higher than the peak for Cl^-. Moreover, the average number of Cl^- adsorbed at the graphite surface, defined as the number of Cl^- with z positions less than z_C, is only 40.3 and is smaller than the corresponding value of 48.0 for Na^+. This leads to the solution, especially near the liquid-gas surface, having negatively charged behavior since there is more Cl^- floated in the solution. As shown in Figure 1D, without the hydrated Na^+-π interactions, Cl^- also has only a flat distribution along the z-direction.

We also performed simulations for systems with different amounts of NaCl solution at the same concentration. Figure 2C shows the average numbers of Na^+ and Cl^- adsorbed on the graphite surface and floated in the solution. We can see that the numbers of Na^+ and Cl^- adsorbed on the surface are saturated with a total number of NaCl, $N = 70$. It should be noted that all Na^+ are adsorbed on the surface, but some Cl^- still float in the solution, $N = 30$; this results in a significant negatively charged behavior in the solution and gas-solution interface. The numbers of Na^+ and Cl^- floated in the solution increase as N increases. From $N = 110$, the amounts of Na^+ and Cl^- floated in the solution are larger than those adsorbed on the surface. This indicates that the accumulation of ions on the surface will largely reduce the ion distribution in the solution and gas-liquid interface, especially for small nanoscale systems.

The adsorption of Na^+ and Cl^- on the graphite surface in the NaCl solution is robust. We performed new simulations with smaller values of ε, i.e., $\varepsilon = \varepsilon_0/2$ and $\varepsilon = \varepsilon_0/4$. As shown in Figure 1C and 1D, the peaks are still clear for both values of ε; the peak heights only decrease about one third value for $\varepsilon = \varepsilon_0/2$. For Na^+, the height of the peak only decreases a little when the values of ε decrease from ε_0 to $\varepsilon_0/2$. Correspondingly, the height of the distribution probability of Na^+ increases slightly over the graphite surface distance $z > 0.5$ nm. We can see a significant decrease in the peak height for $\varepsilon = \varepsilon_0/4$ and a clear increase in the distribution probabilities for $z > 0.42$ nm. For Cl^-, as shown in Figure 1D, we can see a little change in the peak when the values of ε decrease from ε_0 to $\varepsilon_0/2$. The peak height decreases to its quarter value for $\varepsilon = \varepsilon_0/4$. In other words, Na^+ and Cl^- are still abundant on the graphite surface when the adsorption energy ε is reduced to half ε_0, even one-quarter ε_0.

The adsorption of cations on the graphite surface is universal, in that other cations have similar behavior as Na^+. We performed DFT computations of the other cations (Li^+, K^+, Mg^{2+}, Ca^{2+}, Fe^{2+}, Co^{2+}, Cu^{2+}, Cd^{2+}, Cr^{2+}, and Pb^{2+}) on the graphite surface, as shown in Figure 3. We find that the adsorption energy of K^+ is the smallest, at 28.7 kcal/mol, and still reaches 48.1 k_BT at T = 300 K, indicating that all of these metal ions can be adsorbed on the surface at room temperature. We note that the adsorption stability of divalent cations is significantly stronger than that of monovalent cations, so we expect that the graphite surface has a special adsorbing capability for heavy cations, such as Fe^{2+}, Co^{2+}, Cu^{2+}, Cd^{2+}, and Cr^{2+}, which are common heavy metal pollutants in soil and water.

In summary, with a careful consideration of the cation-π interaction, we conclude that Na^+ is enrichment on the typical hydrophobic carbon-based surface with the π electron-rich structures in aqueous salt solutions. Although the interaction of hydrated Cl^- with the carbon-based surface is weak, the electrostatic Na^+-Cl^- interaction also enriches Cl^- at the interface. The average number of Na^+ adsorbed at the graphite surface is significantly higher than that of Cl^-, which results in more Cl^- floated in the solution. We emphasize that, in nanoscale systems, a small total number of ions leads to a significant negatively charged behavior in the solution and enhances the negative charge at the liquid-gas interface.

These observations are robust in that similar results are obtained even when the strength of the hydrated Na^+-π interaction is reduced to half of the original values in the numerical simulations. We note that other cations (Li^+, K^+, Mg^{2+}, Ca^{2+}, Fe^{2+}, Co^{2+}, Cu^{2+}, Cd^{2+}, Cr^{2+}, and Pb^{2+}) have similar behavior to Na^+, in that the cations adsorb on the carbon-based surface with π electron-rich structures.

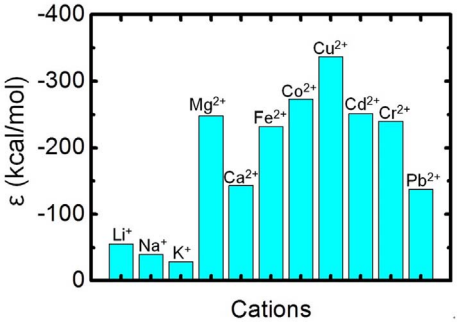

Figure 3 | Adsorption energies of various cations on the graphite surface.

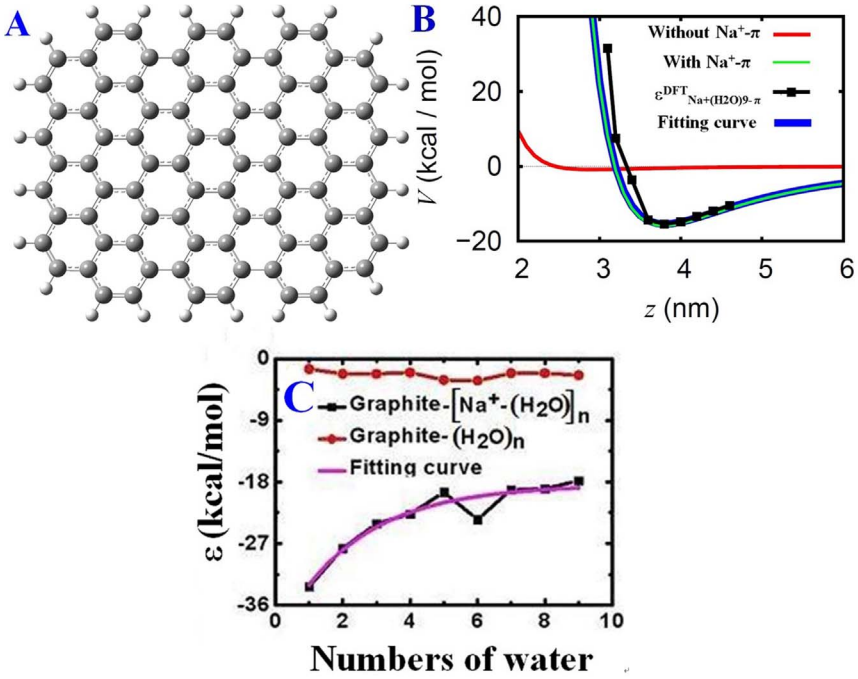

Figure 4 | (A) Schematic description of a two-dimensional graphite surface ($C_{84}H_{24}$) of 12.275 × 15.658 Å^2 (84 carbon atoms and 24 hydrogen atoms). (B) The interaction potential between Na^+ and graphite surface (red line) in the present well-used force field (CHARMM) without including Na^+-π interactions. The adsorption energies of Na^+ with nine water molecules on the graphite surface (black square) on the different distance (z, the vertical dimension between the Na^+ and the surface) at the B3LYP/6–31 G(d) level and the fitting (blue line) potential. The interaction potential between Na^+ and graphite surface (green line) in our used force field incorporated Na^+-π interactions to CHARMM force field. (C) Hydrated Na^+-π interactions energies ε (black squares) and fitting curve (pink line) and the H_2O-π interactions energies ε (red filled circles).

These findings provide new insight into the understanding and control of surface-charged behaviors, and they may lead to potential applications such as ion storage and detection, carbon nanotube-based water purification, graphene-based ion filtration, and bio-related processes. Finally, we note that graphite surfaces have a wonderful adsorbing capability for heavy cation pollution, such as Fe^{2+}, Co^{2+}, Cu^{2+}, Cd^{2+}, and Cr^{2+}, indicating that a low-cost carbon-based material with π electron-rich structures may have widespread potential for dealing with water or soil pollution from heavy metals.

Methods

The B3LYP[54,55] method in the framework of DFT, which have been widely used in the study of water molecules on solid surfaces or inside carbon nanotubes[52,56,57], is used to study the intermolecular interactions. For geometry optimizations, the double-ζ basis is employed, and a d-polarization function is added (marked with 6–31 G(d)). At the same time, the pseudopotential function with Lanl2dz is introduced into the basis set for some metal ions (Fe^{2+}, Co^{2+}, Cu^{2+}, Cd^{2+}, Cr^{2+} and Pb^{2+}). A two-dimensional graphite surface of 12.275 × 15.658 Å^2 is used for the DFT study as shown in Figure 4A, which is large enough to obtain results with a tolerable error, whereas the detailed discussions are shown in our former article[52]. All calculations are carried out using the Gaussian-03 program (Revision D.01, details in Supplementary Information).

The cation-π interactions between Na^+ and the graphite surface are represented by a model potential in the classical MD simulation. Here, we fitted the overall profile a Na^+ with nine water molecules separating the nonpolar hydrophobic graphite surface, as shown in Figure 4B. The fitted potential function presents in Equation 1, where the parameters ε and z_m are the adsorption energy and balance position distance (the vertical dimension between the Na^+ and the surface) of Na^+ with the graphite surface and z is the distance of the vertical dimension between the Na^+ and the surface, which are the main potential parameters describing the cation-π interaction. The z_m = 3.8 Å and ε = ε_0 = −16.4 kcal/mol are used, corresponding to the case of a Na^+ with nine water molecules adsorbed on the graphite surface (see Figure 4C, detailed computation can be found in the Supplementary Information). These cation-π interactions of Na^+ with the nonpolar hydrophobic graphite surfaces were added in MD dynamics simulations programs. Figure 4B shows the present well-used force field (CHARMM) without including Na^+-π interactions, our used force field incorporated Na^+-π interactions to CHARMM force field and the DFT computational results as well as its fitting curve. The DFT computational results are much larger than the present well-used force field obtained if the Na^+-π interaction is neglected and our used force field incorporated Na^+-π interactions to CHARMM force field is consistent with the DFT computational results.

Molecular dynamics simulations are carried out using the program NAMD2/VMD1.9 packages[58], with the CHARMM force field[46], at time steps of 2 fs with the O-H bonds and C atoms held fixed. The TIP3P water model[59] is used with parameters of ε_{OO} = 0.152 kcal/mol, ε_{OH} = 0.084 kcal/mol, ε_{HH} = 0.046 kcal/mol, σ_{OO} = 3.15 Å, σ_{OH} = 1.77 Å and σ_{HH} = 0.40 Å, respectively. The carbon atoms are modeled as uncharged Lennard-Jones particles with parameters of σ_{CC} = 3.55 Å and ε_{CC} = 0.070 kcal mol^{-1}. Na^+ and Cl^- ions are assigned charge to 1.0 e and −1.0 e, respectively, with Lennard-Jones parameters of σ_{NaNa} = 2.43 Å, σ_{ClCl} = 4.04 Å, ε_{NaNa} = 0.047 kcal mol^{-1} and ε_{ClCl} = 0.150 kcal mol^{-1}. The Lennard-Jones parameters of water-ions are ε_{ONa} = 0.084 kcal/mol, ε_{OCl} = 0.151 kcal/mol, ε_{HNa} = 0.046 kcal/mol, ε_{HCl} = 0.083 kcal/mol, σ_{ONa} = 2.79 Å, σ_{OCl} = 3.60 Å, σ_{HNa} = 1.41 Å and σ_{HCl} = 2.22 Å, respectively. In order to speed up computation, the particle-mesh Ewald method with a grid spacing on 1 Å or less is used to full electrostatic interactions computation, while the van der Waals (vdW) interactions are shifted smoothly at 12.0 Å. and constant-volume molecular dynamics simulation is performed. The simulations are performed at NVT with a constant-temperature (300 K) and a Langevin damping coefficient 5 ps^{-1}. The selection of a vapor-liquid coexistence system is used to maintain the ambient condition. Periodic boundary conditions are applied in all directions.

For the NaCl solution, the initial simulation box size is Lx = 4.2 nm, Ly = 4.2 nm, and Lz = 20.000 nm, where Lz is set to be sufficiently large to eliminate the image effect in the z direction. During the simulations, we fix the graphite surface, which contains two layers graphite and there are 598 carbon atoms of every layer, and every carbon-carbon bond is 1.420 Å. All of Na^+, Cl^- and water molecules are free to move in this simulation. All systems are equilibrated for 4 ns.

1. Ma, J. C. & Dougherty, D. A. The Cation-π Interaction. *Chem. Rev.* **97**, 1303–1324 (1997).
2. Kogut, B. M. Assessment of the Humus Content in Arable Soils of Russi. *Eur. Soil Sci.* **35**, 843–851 (2012).
3. Piccolo, A. The Supramolecular Structure of Humic Dubstances. A Novel Understanding of Humus Chemistry and Implications in Soil Science. *Adv. Agron.* **75**, 57–134 (2002).
4. Hitzel, A., Pöhlmann, M., Schwägele, F., Speer, K. & Jira, W. Polycyclic Aromatic Hydrocarbons (PAH) and Phenolic Substances in Meat Products Smoked with Different Types of Wood and Smoking Spices. *Food Chem.* **139**, 955–962 (2013).
5. Fetzer, J. C. The Chemistry and Analysis of the Large Polycyclic Aromatic Hydrocarbons. *Polycycl. Aromat. Comp.* **27**, 143–162 (2000).
6. Larsson, B. K., Sahlberg, G. P., Eriksson, A. T. & Busk, L. A. Polycyclic Aromatic Hydrocarbons in Grilled Food". *J. Agric. Food Chem.* **31**, 867–873 (1983).

7. Liu, Y., Dong, X. & Chen, P. Biological and Chemical Sensors Based on Graphene Materials. *Chem. Soc. Rev.* **41**, 2283–2307 (2012).
8. Shi, G., Ding, Y. & Fang, H. Unexpectedly Strong Anion–π Interactions on the Graphene Flakes. *J. Comput. Chem.* **33**, 1328–1337 (2012).
9. Hummer, G., Rasaiah, J. C. & Noworyta, J. P. Water Conduction through the Hydrophobic Channel of a Carbon Nanotube. *Nature* **414**, 188–190 (2001).
10. Chan, S., Chen, G., Gong, X. G. & Liu, Z. Oxidation of Carbon Nanotubes by Singlet O_2. *Phys. Rev. Lett.* **90**, 086403 (2003).
11. García-Hernández, D. A., Manchado, A., García-Lario, P., Stanghellini, L., Villaver, E. *et al.* "Formation of Fullerenes in H-Containing Planatary Nebulae" *Astrophys. J. Lett.* **724**, 39–43 (2010).
12. Roger, K. & Cabane, B. Why Are Hydrophobic/Water Interfaces Negatively Charged? *Angew. Chem., Int. Ed.* **51**, 5625–5628 (2012).
13. Tian, C. S. & Shen, Y. R. Structure and Charging of Hydrophobic Material/Water Interfaces Studied by Phase-sensitive Sum-Frequency Vibrational Spectroscopy. *Proc. Natl. Acad. Sci. USA* **106**, 15148–15153 (2009).
14. Kudin, K. N. & Car, R. Why Are Water-Hydrophobic Interfaces Charged? *J. Am. Chem. Soc.* **130**, 3915–3919 (2008).
15. Horinek, D. & Netz, R. R. Specific Ion Adsorption at Hydrophobic Solid Surfaces. *Phys. Rev. Lett.* **99**, 226104 (2007).
16. dos Santos, A. P. & Levin, Y. Ion Specificity and the Theory of Stability of Colloidal Suspensions. *Phys. Rev. Lett.* **106**, 167801 (2011).
17. Wong, K., Mukherjee, B., Kahler, A. M., Zepp, R. & Molina, M. Influence of Inorganic Ions on Aggregation and Adsorption Behaviors of Human Adenovirus. *Environ. Sci. Technol.* **46**, 11145–11153 (2012).
18. Madaeni, S. S. & Heidary, F. Effect of Surface Modification of Microfiltration Membrane on Capture of Toxic Heavy Metal Ions. *Environ. Technol.* **33**, 393–399 (2012).
19. Baniamerian, M. J., Moradi, S. E., Noori, A. & Salahi, H. The Effect of Surface Modification on Heavy Metal Ion Removal from Water by Carbon Nanoporous Adsorbent. *Appl. Sur. Sci.* **256**, 1347–1354 (2009).
20. Park, S. & Ruoff, R. S. Chemical Methods for the production Graphenes. *Nat. Nanotech.* **4**, 217–224 (2009).
21. Wu, J., Pisula, W. & Müllen, K. Graphene as Potential Material for electronics. *Chem. Rev.* **107**, 718–747 (2007).
22. Nostro, P. Lo. & Ninham, B. W. Hofmeister Phenomena: An Update on Ion Specificity in Biology. *Chem. Rev.* **112**, 2286–2322 (2012).
23. Drew, K. R. P., Sanders, L. K., Culumber, Z. W., Zribi, O. & Wong, G. C. L. Cationic Amphiphiles Increase Activity of Aminoglycoside Antibiotic Tobramycin in the Presence of Airway Polyelectrolytes. *J. Am. Chem. Soc.* **131**, 486–493 (2009).
24. Lund, M., Jungwirth, P. & Woodward, C. E. Ion Specific Protein Assembly and Hydrophobic Surface Forces. *Phys. Rev. Lett.* **100**, 258105 (2008).
25. Levin, Y., dos Santos, A. P. & Diehl, A. Ions at the Air-Water Interface: An End to a Hundred-Year-Old Mystery? *Phys. Rev. Lett.* **103**, 257802 (2009).
26. Jungwirth, P. & Tobias, D. J. Specific Ion Effects at the Air/Water Interface. *Chem. Rev.* **106**, 1259–1281 (2006).
27. Ghosal, S., Hemminger, J. C., Bluhm, H., Mun, B. S., Hebenstreit, E. L. D. *et al.* Electron Spectroscopy of Aqueous Solution Interfaces Reveals Surface Enhancement of Halides. *Science* **307**, 563–566 (2005).
28. Garrett, B. C. Ions at the Air/Water Interface. *Science* **303**, 1146–1147 (2004).
29. Finlayson-Pitts, B. J. The Tropospheric Chemistry of Sea Salt: A Molecular-Level View of the Chemistry of NaCl and NaBr. *Chem. Rev.* **103**, 4801–4822 (2003).
30. Laskin, A., Gaspar, D. J., Wang, W., Hunt, S. W., Cowin, J. P. *et al.* Reactions at Interfaces As a Source of Sulfate Formation in Sea-Salt Particles. *Science* **301**, 340–344 (2003).
31. Oh, K. J., Gao, G. T. & Zeng, X. C. Nucleation of Water and Methanol Droplets on Cations and Anions: The Sign Preference. *Phys. Rev. Lett.* **86**, 5080 (2001).
32. Park, C., Fenter, P. A., Nagy, K. L. & Sturchio, N. C. Hydration and Distribution of Ions at the Mica-Water Interface. *Phys. Rev. Lett.* **97**, 016101 (2006).
33. Sunner, J., Nishizawa, K. & Kebarle, P. Ion-solvent molecule interactions in the gas phase. The potassium ion and benzene. *J. Phys. Chem.* **85**, 1814–1820 (1981).
34. Mahadevi, A. S. & Sastry, G. N. Cation-π interactions: Its role and relevance in chemistry, biology, and material science. *Chem. Rev.* **113**, 2100–2138 (2013).
35. Dougherty, D. A. The cation-π interaction. *Acc. Chem. Res.* **46**, 885–893 (2013).
36. Daze, K. D. & Hof, F. The cation-π interaction at protein-protein interaction interfaces: developing and learning from synthetic mimics of proteins that bind methylated lysines. *Acc. Chem. Res.* **46**, 937–945 (2013).
37. Duan, M., Song, B., Shi, G., Li, H., Ji, G. *et al.* Cation⊗3π: cooperative interaction of a cation and three benzenes with an anomalous order in binding energy. *J. Am. Chem. Soc.* **134**, 12104–12109 (2012).
38. Song, B., Yang, J., Zhao, J. & Fang, H. Intercalation and Diffusion of Lithium Ions in a Carbon Nanotube Bundle by *ab initio* Molecular Dynamics Simulations. *Energy Environ. Sci.* **4**, 1379–1384 (2011).
39. Knowles, R. R. & Jacobsen, E. N. Attractive Noncovalent Interactions in Asymmetric Catalysis: Links between Enzymes and Small Molecule Catalysts. *Proc. Natl. Acad. Sci. USA* **107**, 20678–20685 (2010).
40. Wang, R. & Xie, T. Macroscopic Evidence of Strong Cation–π Interactions in a Synthetic Polymer System. *Chem. Commun.* **46**, 1341–1343 (2010).
41. Xiu, X., Puskar, N. L., Shanata, J. A. P., Lester, H. A. & Dougherty, D. A. Nicotine binding to brain receptors requires a strong cation-π interaction. *Nature* **458**, 534–538 (2009).
42. Lu, Z., Lai, J. & Zhang, Y. Importance of Charge Independent Effects in Readout of the Trimethyllysine Mark by HP1 Chromodomain. *J. Am. Chem. Soc.* **131**, 14928–14931 (2009).
43. Torrice, M. M., Bower, K. S., Lester, H. A. & Dougherty, D. A. Probing the Role of the Cation–π Interaction in the Binding Sites of GPCRs using Unnatural Amino Acids. *Proc. Natl. Acad. Sci. U.S.A.* **106**, 11919–11924 (2009).
44. Hu, J., Barbour, L. J. & Gokel, G. W. Probing Alkali Metal–π Interactions with the Side Chain Residue of Tryptophan. *Proc. Natl. Acad. Sci. U.S.A.* **99**, 5121–5126 (2002).
45. Jorgensen, W. L., Chandrasekhar, J., Madura, J. D., Impey, R. W. & Klein, M. L. Comparison of Simple Potential Functions for Simulating Liquid Water. *J. Chem. Phys.* **79**, 926 (1983).
46. MacKerell, A. D., Bashford, D., Bellott, M., Dunbrack, R. L., Evanseck, J. D. *et al.* All-Atom Empirical Potential for Molecular Modeling and Dynamics Studies of Proteins. *J. Phys. Chem. B* **102**, 3586–3616 (1998).
47. Jorgensen, W. L., Maxwell, D. S. & Tirado-Rives, J. Development and Testing of the OPLS All-Atom Force Field on Conformational Energetics and Properties of Organic Liquids. *J. Am. Chem. Soc.* **118**, 11225–11236 (1996).
48. García-Fandiño, R. & Sansom, M. S. P. Designing biomimetic pores based on carbon nanotubes. *Proc. Natl. Acad. Sci. U.S.A.* **109**, 6939–6944 (2012).
49. Cohen-Tanugi, D. & Grossman, J. C. Water Desalination across Nanoporous Graphene. *Nano Lett.* **12**, 3602–3608 (2012).
50. Kyaw Sint, Boyang Wang & Petr Král. Selective Ion Passage through Functionalized Graphene Nanopores. *J. Am. Chem. Soc.* **130**, 16448–16449 (2008).
51. Corry, B. Designing Carbon Nanotube Membranes for Efficient Water Desalination. *J. Phys. Chem. B* **112**, 1427–1434 (2008).
52. Shi, G. S., Wang, Z. G., Zhao, J. J., Hu, J. & Fang, H. P. Adsorption of sodium ions and hydrated sodium ions on the hydrophobic graphite surface via cation-π interactions. *Chin. Phys. B* **20**, 068101 (2011).
53. Schyman, P. & Jorgensen, W. L. Exploring Adsorption of Water and Ions on Carbon Surfaces Using a Polarizable Force Field. *J. Phys. Chem. Lett.* **4**, 468–474 (2013).
54. Becke, A. D. Density-Functional Exchange-Energy Approximation with Correct Asymptotic Behavior. *Phys. Rev. A* **38**, 3098 (1988).
55. Lee, C., Yang, W. & Parr, R. G. Development of the Colle-Salvetti Correlation-Energy Formula into a Functional of the Electron Density. *Phys. Rev. B* **37**, 785 (1988).
56. Cicero, G., Grossman, J. C., Schwegler, E., Gygi, F. & Galli, G. Water confined in nanotubes and between graphene sheets: a first principle study. *J. Am. Chem. Soc.* **130**, 1871–1878 (2008).
57. Meng, S., Zhang, Z. & Kaxiras, E. Tuning Solid Surfaces from Hydrophobic to Superhydrophilic by Submonolayer Surface Modification. *Phys. Rev. Lett.* **97**, 036107 (2006).
58. Phillips, J. C., Braun, R., Wang, W., Gumbart, J., Tajkhorshid, E. *et al.* Scalable Molecular Dynamics with NAMD. *J. Comput. Chem.* **26**, 1781–1802 (2005).
59. Jorgensen, W. L., Chandrasekhar, J., Madura, J. D., Impey, R. W. & Klein, M. L. Comparison of Simple Potential Functions for Simulating Liquid Water. *J. Chem. Phys.* **79**, 926 (1983).

Acknowledgments

We thank Drs. Yihong Ding, Shen Wang, Nan Sheng, Wenpeng Qi, Rongzheng Wan, Xiaoling Lei, Jiang Li, Qing Ji, Jijun Zhao, and Teng Yang for their constructive suggestions. This work is supported by the National Science Foundation of China under grant No. 11290164, and 11204341, the Shanghai Natural Science Foundation of China under grant No. 13ZR1447900, the Knowledge Innovation Program of SINAP, the Supercomputer Center of Chinese Academy of Sciences and the Shanghai Supercomputer Center of China.

Author contributions

G.S. and J.L. performed most of the numerical simulations. H.F. and G.S. carried out most of the theoretical analysis. C.W., B.S., Y.T. and J.H. carried out some theoretical analysis. H.F. and G.S. contributed most of the ideas and wrote the paper. All authors discussed the results and commented on the manuscript.

Additional information

Supplementary information accompanies this paper at http://www.nature.com/scientificreports

Competing financial interests: The authors declare no competing financial interests.

How to cite this article: Shi, G.S. *et al.* Ion Enrichment on the Hydrophobic Carbon-based Surface in Aqueous Salt Solutions due to Cation-π Interactions. *Sci. Rep.* **3**, 3436; DOI:10.1038/srep03436 (2013).